

# Many-body quantum non-Markovianity

Jonathan Brugger,<sup>1,2</sup> Christoph Dittel,<sup>1,2</sup> and Andreas Buchleitner<sup>1,2</sup>

<sup>1</sup>*Physikalisches Institut, Albert-Ludwigs-Universität Freiburg,  
Hermann-Herder-Straße 3, 79104 Freiburg, Germany*

<sup>2</sup>*EUCOR Centre for Quantum Science and Quantum Computing, Albert-Ludwigs-Universität Freiburg,  
Hermann-Herder-Straße 3, 79104 Freiburg, Germany*

(Dated: July 14, 2022)

We port the concept of non-Markovian quantum dynamics to the many-particle realm, by a suitable decomposition of the many-particle Hilbert space. We show how the specific structure of many-particle states determines the observability of non-Markovianity by single- or many-particle observables, in a readily implementable few-particle set-up.

Non-Markovian behavior [1] is the partial restoration of an open quantum system's memory of its past. In general, we expect that an open quantum system – widely (though not exclusively) understood as living on a small number of degrees of freedom, as opposed to the many degrees of freedom of an environment or bath it is coupled to – tends to irreversibly lose its memory, since any information leaking to the environment will quickly disperse and not relocalize on the system degrees of freedom [2–4]. However, this intuition is reliable only in the case where the number of degrees of freedom associated with system and environment, as well as the associated spectral structures, are distinct, and when system and environment degrees of freedom do not easily entangle. Consequently, non-Markovian behavior is naturally expected, e.g., in large molecular structures [5–9] where different degrees of freedom are strongly coupled and typically non-separable, with the consequence that Markovian master equation-like descriptions (very successfully employed for many quantum optical applications [2]) turn unreliable. Given the ever improving experimental resolution of the dynamics of diverse multi-component quantum systems [10–15], there is a strong incentive to improve our understanding of non-Markovianity, and to identify observables which allow for an unambiguous identification of non-Markovian effects.

While the intuition underlying non-Markovian behavior has been clear for long [2, 3], the concept has been formalized, and many of its subtleties clarified [1, 16–22], during recent years. We here rely on the definition and quantification of non-Markovian behavior in terms of information back-flow from the environment into the system degrees of freedom, as formalized through the time dependence of the trace distance [1, 17]

$$D(\rho, \sigma) = \frac{1}{2} \text{tr} |\rho - \sigma| \quad (1)$$

of initially distinct system states  $\rho$  and  $\sigma$ , with  $|M| = \sqrt{MM^\dagger}$  the positive square root of a positive semi-definite operator. Since a metric on the space of density matrices, with  $D(\rho, \sigma) = 0$  if and only if  $\rho = \sigma$ , and  $D(\rho, \sigma) = 1$  if and only if  $\rho$  and  $\sigma$  have orthogonal support [1], the trace distance is an exhaustive mea-

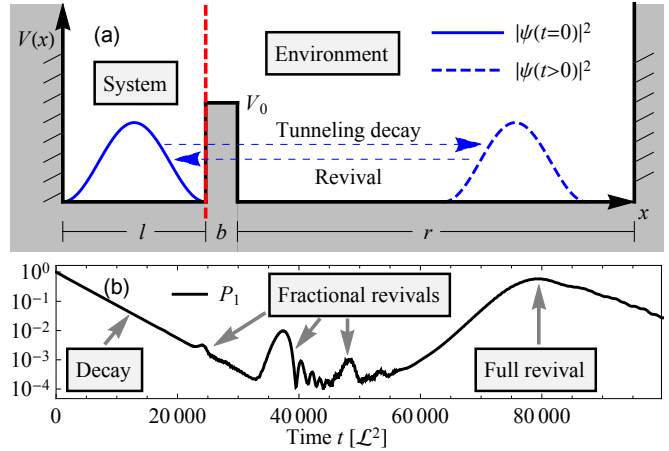


FIG. 1. Tunneling dynamics in a one-dimensional asymmetric double-well potential. (a) Sketch: A particle prepared (continuous blue line,  $|\psi(t = 0)|^2$ ) in the left well (system) tunnels into the right well (environment), is reflected at the right boundary, and possibly re-enters the system (dashed blue line,  $|\psi(t > 0)|^2$ ). (b) Semilogarithmic plot of the probability  $P_1$  for a single particle, initially prepared in the ground state  $|1\rangle$  of the isolated system, to be found in the system (left well), for the parameters  $l = 50 \mathcal{L}$ ,  $b = 2 \mathcal{L}$ ,  $r = 4000 \mathcal{L}$  and  $V_0 = 0.1 \mathcal{L}^{-2}$ .

sure for the distinguishability of two quantum states – by any type of measurement – and, thus, of their distinctive information content. However, when state tomography turns unaffordable, e.g. due to the underlying Hilbert space dimension [23], it is a priori often unclear which observable can expose such distinctive information most efficiently, and particularly so when dealing with many-particle states.

Intuitively, though, information flow is easily associated with the exchange of excitations in different degrees of freedom, and we will here build on this intuition by considering the specific – and experimentally feasible [24] – example of few fermions or bosons loaded into the asymmetric, one-dimensional double-well potential depicted in Fig. 1(a): Left and right potential wells of width  $l$  and  $r$  each define local mode structures which we associate with the system's and environmental degrees

of freedom, respectively. They are separated by a finite rectangular barrier of width  $b$  and height  $V_0$ , which is considered as part of the environment. As shown earlier [25–27], this model allows an exact spectral treatment of the decay dynamics of an open many-body system with a continuously tunable, discrete to quasi-continuous spectral structure of the environment. System-environment coupling is determined by  $b$  and  $V_0$ , and weak coupling and a quasi-continuous spectrum of the environment, in the limit of large  $r$ , justify the intuition of the system being opened to couple to the environment's degree of freedom. While we will elaborate elsewhere [28] on how to control non-Markovian dynamics by tuning, through variable  $r$ , the transition to a quasi-continuum, we here focus on a fixed, finite width  $r$ , which generates the typical behavior. In all subsequent simulations we choose the parameters  $l = 50\mathcal{L}$ ,  $b = 2\mathcal{L}$ ,  $r = 4000\mathcal{L}$  and  $V_0 = 0.1\mathcal{L}^{-2}$  (all measured in terms of the characteristic experimental length scale  $\mathcal{L}$  [26]), which, in particular, establish the quasi-continuous limit for the environment's spectrum (notwithstanding the hard-wall boundary condition of the right well's outer confinement, which clearly induces non-Markovian behavior on sufficiently long time scales [26, 27]).

We seed the unitary dynamics of system and environment by the initial preparation of a single- or many-particle eigenstate of the isolated (i.e.,  $V_0 \rightarrow \infty$ ) left well. The single-particle dynamics are obtained via spectral decomposition, with the single-particle eigenstates extracted from exact numerical diagonalization [28] of the single-particle Hamiltonian  $H_{\text{sp}}(x) = -\partial^2/\partial x^2 + V(x)$  (in natural units, with  $\hbar \equiv 1$  and mass  $m \equiv 1/2$ ), after discretization in a suitable finite element basis [29, 30]. We further equip the particles with an internal degree of freedom with  $\mathcal{H}_{\text{int}} = \text{span}\{|+\rangle, |-\rangle\}$ , not coupled to their external degree of freedom (i.e., their position within the double well). In particular,  $H_{\text{sp}}(x)$  is independent of the particle's internal state. In our present discussion we restrict ourselves to non-interacting particles, such that many-particle eigenstates are (anti-) symmetrized product states of single-particle eigenstates. The numerically more elaborate case of interacting particles will be investigated elsewhere [28]. However, all conceptional observations and analytical results stated hereafter apply for arbitrary strength and type of the interaction.

The dynamics of a single particle in the double-well potential can be conceived in the Hilbert space  $\mathcal{H} = \mathcal{H}_{\text{S}} \oplus \mathcal{H}_{\text{E}}$ , with  $\mathcal{H}_{\text{S(E)}}$  representing the system (environment). Note that  $\mathcal{H}$  is given by a direct sum, such that any pure state of the total system can be written as  $|\psi\rangle = c_1 \Pi_{\text{S}} |\psi\rangle + c_0 \Pi_{\text{E}} |\psi\rangle$ , with  $\Pi_{\text{S(E)}}$  the projector onto  $\mathcal{H}_{\text{S(E)}}$ , and the probability  $P_1 = |c_1|^2$  to find the particle in (any eigenstate of) the (isolated) system. Figure 1(b) shows the time evolution of  $P_1$  after initializing the particle in the ground state  $|1\rangle$  of the isolated system. We observe an exponential decay, followed by

low-amplitude (note the semi-logarithmic scale) partial (fractional) [31, 32] revivals, and, subsequently, a pronounced full revival. Fractional and full revivals are due to the coherent superposition of single particle amplitudes reflected at the barrier and at the right boundary of the environment, with an admixture of non-vanishing excited state amplitudes of the system degree of freedom. The latter define the fractional revival times in Fig. 1(b), and are individually enhanced when launching the dynamics in an excited system state, as, e.g.,  $|2\rangle$  in Fig. 2(a). Since such revivals express excitation and, thus, information backflow into the system degree of freedom, they are indicative of non-Markovianity, as we quantify further down.

Let us, however, first turn towards the general many-particle problem. The many-particle dynamics of any number  $N$  of identical bosons (fermions) play in the Fock space  $\Gamma^{\text{b(f)}}(\mathcal{H})$  [33], which is constructed from the single-particle Hilbert space  $\mathcal{H} = \mathcal{H}_{\text{S}} \oplus \mathcal{H}_{\text{E}}$ , and can be factorized as a tensor product [34, 35],

$$\Gamma^{\text{b(f)}}(\mathcal{H}_{\text{S}} \oplus \mathcal{H}_{\text{E}}) \cong \Gamma^{\text{b(f)}}(\mathcal{H}_{\text{S}}) \otimes \Gamma^{\text{b(f)}}(\mathcal{H}_{\text{E}}). \quad (2)$$

The fact that we consider unitary dynamics and a well-defined particle number on the combined system and environment degrees of freedom restricts the time evolution to the effective  $N$ -particle space

$$\mathcal{H}_{\text{eff}}^N = \bigoplus_{k=0}^N \left( \mathcal{H}_{\text{S}}^{\otimes k} \otimes \mathcal{H}_{\text{E}}^{\otimes (N-k)} \right)_{\text{s(a)}} \subset \Gamma^{\text{b(f)}}(\mathcal{H}), \quad (3)$$

where  $\mathcal{H}_{\text{s(a)}}$  denotes the (anti-) symmetrization of the Hilbert space  $\mathcal{H}$ . As a consequence, every pure state of system and environment can be written as  $|\psi\rangle = \sum_{k=0}^N c_k |\psi_k\rangle \in \mathcal{H}_{\text{eff}}^N$ , with  $|\psi_k\rangle$  a state with  $k$  out of  $N$  particles confined to the modes of the system. To assess the non-Markovian character of the system dynamics, we need to trace  $|\psi\rangle$  over the environment, to produce the reduced system state

$$\rho_{\text{S}} = \text{tr}_{\text{E}} |\psi\rangle\langle\psi| = \sum_{k=0}^N |c_k|^2 \rho_k, \quad (4)$$

with  $\rho_k = \text{tr}_{\text{E}} |\psi_k\rangle\langle\psi_k|$ .  $\rho_{\text{S}}$  exhibits block-diagonal structure, since states of the environment corresponding to different particle numbers are orthogonal [28].

The trace distance  $D(\rho_{\text{S}}, \sigma_{\text{S}})$  between two reduced states  $\rho_{\text{S}} = \sum_k |c_k|^2 \rho_k$  and  $\sigma_{\text{S}} = \sum_k |d_k|^2 \sigma_k$  of the system can now be evaluated for arbitrary particle number, particle type (bosons or fermions), degree of (in-) distinguishability and interaction strength, as  $D(\rho_{\text{S}}, \sigma_{\text{S}}) = \sum_{k=0}^N D(|c_k|^2 \rho_k, |d_k|^2 \sigma_k)$ . Whenever  $D(\rho_{\text{S}}, \sigma_{\text{S}})$  increases as a function of time, this signals non-Markovian behaviour. Although the block-diagonal structure of  $\rho_{\text{S}}$  and  $\sigma_{\text{S}}$  significantly reduces the computational complexity of the trace distance  $D(\rho_{\text{S}}, \sigma_{\text{S}})$ , it remains non-trivial to

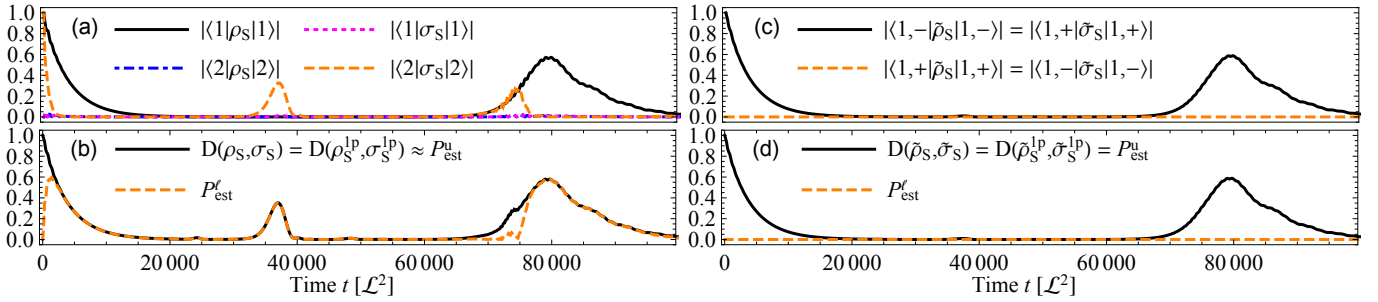


FIG. 2. Non-Markovian single-particle tunneling in an asymmetric double-well potential (see Fig. 1). The revivals (a) of the auto- ( $|\langle 1|\rho_s|1\rangle|$ ,  $|\langle 2|\sigma_s|2\rangle|$ ) and cross correlation functions ( $|\langle 2|\rho_s|2\rangle|$ ,  $|\langle 1|\sigma_s|1\rangle|$ ) of a single particle initially prepared in the ground state  $|1\rangle$  or in the first excited state  $|2\rangle$ , respectively, of the isolated left potential well and reduced to the system (i.e., the left well's) degrees of freedom are faithfully reflected by the trace distance  $D(\rho_s, \sigma_s)$ , Eq. (1), as well as, almost everywhere, by its estimators (6,7,9) ( $P_{\text{est}}^u \approx D(\rho_s, \sigma_s)$  [28], with deviations smaller than  $10^{-2}$ ). Only at  $t \approx 74000 \mathcal{L}^2$  is the lower bound  $P_{\text{est}}^\ell$ , Eq. (6), not tight, since it does not resolve single state population differences, but only those of the total particle number probabilities in the left well. For the same reason is  $P_{\text{est}}^\ell$  unable to discriminate single particle states launched in the ground state  $|1\rangle$ , but labeled with mutually orthogonal states  $|\pm\rangle$  in an additional degree of freedom: Only the estimators (7,9) and the trace distance  $D(\tilde{\rho}_s, \tilde{\sigma}_s)$  (d) sense the revivals (c) featured by the autocorrelation functions  $|\langle 1, -|\tilde{\rho}_s|1, -\rangle|$  and  $|\langle 1, +|\tilde{\sigma}_s|1, +\rangle|$ .

evaluate, especially for the dynamics of many *interacting* particles [28]. However, as we show in the following, this burden can often be alleviated by relating the trace distance  $D(\rho_s, \sigma_s)$  to computationally and experimentally more readily accessible quantities.

From Eq. (4) we directly obtain the probability  $P_k(\rho_s) = |c_k|^2$  to find *exactly*  $k$  particles in the system and  $N - k$  particles in the environment. The quantities  $P_k$  constitute simple many-particle observables (given the availability of number-resolving detectors in the lab), and turn out useful in order to distinguish Markovian from non-Markovian many-body dynamics. A straightforward calculation [28] shows that the trace distance is bounded by

$$P_{\text{est}}^\ell \leq D(\rho_s, \sigma_s) \leq P_{\text{est}}^u, \quad (5)$$

with the lower and upper bounds given by

$$P_{\text{est}}^\ell = \sum_{k=0}^N \frac{||c_k|^2 - |d_k|^2|}{2} \quad (6)$$

and

$$P_{\text{est}}^u = 1 - \frac{|c_0|^2 + |d_0|^2|}{2} + \frac{|c_0|^2 - |d_0|^2|}{2}, \quad (7)$$

respectively. Intuitively,  $P_{\text{est}}^\ell$  is the sum of *minimal* trace distances within the blocks in (4), given each by the associated population differences. Analogously,  $P_{\text{est}}^u$  is the sum of the *exact* trace distance in the one-dimensional block  $k = 0$ , and the *maximal* trace distances within all blocks  $k \geq 1$ , again given by population differences.

Similarly, we can bound the trace distance  $D(\rho_s, \sigma_s)$  in terms of single particle observables. To this end we con-

sider the *reduced single-particle density matrix* (RSPDM)

$$\rho_s^{1p} = \text{tr}_{2, \dots, N}(\rho_s) = |c_0|^2 \rho_0 + |c_1|^2 \rho_1 + \sum_{k=2}^N |c_k|^2 \text{tr}_{2, \dots, k} \rho_k \quad (8)$$

obtained from the system's state (4) by tracing out all but one particle [36, 37]. It describes a potentially mixed state with up to one particle in the system and offers a natural way to compare states on a single-particle level, since the expectation value (with respect to  $\rho_s$ ) of any single-particle observable (like, e.g., the projection  $|1\rangle\langle 1|$  onto the single-particle ground state) can be given in terms of the RSPDM [37]. Using the contractivity of the trace distance under trace-preserving quantum operations [38, 39] we find

$$D(\rho_s^{1p}, \sigma_s^{1p}) \leq D(\rho_s, \sigma_s), \quad (9)$$

again bounding the trace distance from below.

Equations (5-9) thus provide bounds on  $D(\rho_s, \sigma_s)$ , and, consequently, on the non-Markovianity of the system dynamics [40], which can be assessed by monitoring simple features of the counting statistics or of single particle observables like the ground state population of the system. Let us inspect the tightness of these bounds for different choices of single- and many-particle states: Fig. 2 (a,b) compares the evolution of the auto- and cross correlation functions of two pure single particle states, launched in the system's ground and first excited states, respectively, upon trace over the environment, to the time evolution of their trace distance. We see that the revival dynamics of the system state populations in (a) is faithfully reflected by the trace distance in (b), and almost everywhere reproduced by the lower bound  $P_{\text{est}}^\ell$ , thus comforting our intuition that information backflow

is synonymous to excitation backflow. However, we also see from the mismatch between  $P_{\text{est}}^\ell$  and  $D(\rho_S, \sigma_S)$  at  $t \simeq 74000 \mathcal{L}^2$ , where both autocorrelation functions revive simultaneously, that  $P_{\text{est}}^\ell$ , which only monitors the population difference in the system, without resolving individual system state populations, is then too coarse grained a quantifier to distinguish both states. Likewise, the reviving trace distance of two pure single particle states both launched in the system's ground state, but labeled by mutually orthogonal states of an additional degree of freedom, is faithfully reproduced by  $P_{\text{est}}^u$  and  $D(\rho_S^{1p}, \sigma_S^{1p})$ , while  $P_{\text{est}}^\ell$  is blind for this distinction, by its very construction. The latter is in contrast to the estimate  $P_{\text{est}}^u$ , which is [approximately] tight in Fig. 2(d) [Fig. 2(b)], as the particles are prepared in and return to [essentially] orthogonal single-particle modes of the system, thus [almost] realizing the maximal trace distance assumed in the derivation of (7).

Let us now inspect how to sense non-Markovianity on the many-particle level: Fig. 3 shows exemplary cases of the trace distance of pairs of time-evolved, reduced fermionic and bosonic few particle system states. Panel (a) monitors the trace distance  $D(\rho_S, |0_S\rangle\langle 0_S|)$  of three non-interacting, indistinguishable fermions, launched in the system ground state, from the (time-invariant) many-particle system vacuum  $|0_S\rangle$ , as well as the trace distance estimates (6,7,9), which here all coincide [28]. Recombination(s) of the three-particle state into the ground, first, and second excited system state, as clearly reflected by the revivals of the reduced state single particle autocorrelation functions  $|\langle j|\rho_S^{1p}|j\rangle|$ , induces non-Markovianity as unambiguously indicated by synchronous revivals of the above distance measures.

Fig. 3 (b) shows the time evolution of the trace distance of bosonic four- and five-particle states launched in the system ground states,  $\tilde{\rho}(0) = \tilde{\rho}_S(0) = |1\rangle\langle 1|^{\otimes 4}$  and  $\tilde{\sigma}(0) = \tilde{\sigma}_S(0) = |1\rangle\langle 1|^{\otimes 5}$ , respectively. Non-Markovianity here stems from a many-particle repopulation of the system ground state, which, due to dispersion within the environment, stretches over a longer time interval, thus leading to an only mild revival of the states' trace distance. The reduced single particle states are barely discriminated by the single particle trace distance, on the rising and on the falling edge of the repopulation of the system ground state, and cannot be distinguished at the maximum of the many-particle revival (by construction).

While the bosonic many-particle states in panel (b) are distinguished by their particle number difference, Fig. 3(c) considers two six-particle states of distinguishable and indistinguishable particles, respectively. These states only differ if at least two particles in different single-particle states populate the system, and we therefore specifically consider  $\hat{\rho}(0) = \hat{\rho}_S(0) = \mathcal{S}(|1\rangle\langle 1|^{\otimes 3} \otimes |2\rangle\langle 2|^{\otimes 3})$  and  $\hat{\sigma}(0) = \hat{\sigma}_S(0) = |1\rangle\langle 1|^{\otimes 3} \otimes |2\rangle\langle 2|^{\otimes 3}$  [41], with initially three particles in each, the ground and first ex-

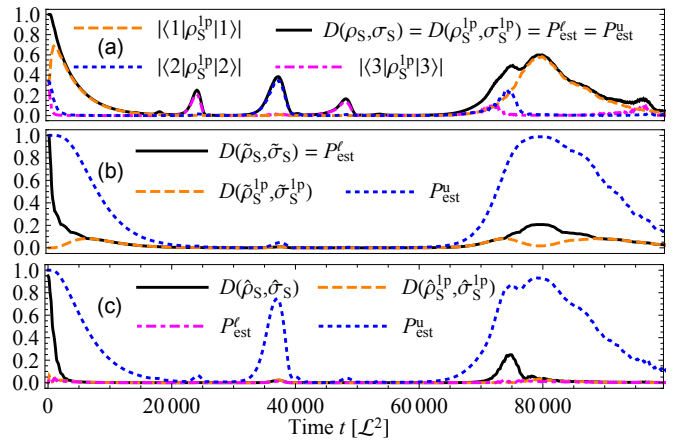


FIG. 3. Non-Markovian many-particle tunneling: (a) Three indistinguishable fermions launched in the (fermionic) ground state of the isolated left well (see Fig. 1) exhibit clear revivals of the reduced single particle autocorrelation functions  $|\langle j|\rho_S^{1p}|j\rangle|$ ,  $j = 1, 2, 3$ , of the left well's ground, first and second excited single particle states. This gives rise to non-Markovian behavior as clearly manifest in the state's trace distance  $D(\rho_S, \sigma_S)$  from the left well's (time-invariant) many-particle vacuum state  $\sigma_S = |0_S\rangle\langle 0_S|$ . The trace distance estimators  $D(\tilde{\rho}_S^{1p}, \tilde{\sigma}_S^{1p})$ ,  $P_{\text{est}}^\ell$ ,  $P_{\text{est}}^u$ , (6,7,9), are tight, due to  $d_k = \delta_{0k}$  for the many-particle vacuum state [28]. (b) and (c) monitor the trace distance and its estimators (6,7,9) for two pairs of bosonic many-particle states: The trace distance  $D(\tilde{\rho}_S^{1p}, \tilde{\sigma}_S^{1p})$  of the reduced single particle states of the four and five particle states launched in the bosonic ground states (b) of the isolated left well,  $\tilde{\rho}(0) = \tilde{\rho}_S(0) = |1\rangle\langle 1|^{\otimes 4}$  and  $\tilde{\sigma}(0) = \tilde{\sigma}_S(0) = |1\rangle\langle 1|^{\otimes 5}$ , respectively, only barely detects the many-body revival in the system ground state. To detect non-Markovianity by comparison of (c) the many-particle dynamics of the six-particle states prepared in  $\hat{\rho}(0) = \hat{\rho}_S(0) = \mathcal{S}(|1\rangle\langle 1|^{\otimes 3} \otimes |2\rangle\langle 2|^{\otimes 3})$  and  $\hat{\sigma}(0) = \hat{\sigma}_S(0) = |1\rangle\langle 1|^{\otimes 3} \otimes |2\rangle\langle 2|^{\otimes 3}$ , respectively, which differ only by their (un-) symmetrized character ( $\mathcal{S}$  the bosonic symmetrization operator), bona fide many-particle observables need to be interrogated.

cited system state, respectively, and  $\mathcal{S}$  the bosonic symmetrization operator. These states can be told apart only from their symmetry properties, by trace distances  $D(\hat{\rho}_S^{kp}, \hat{\sigma}_S^{kp})$  of reduced  $k$ -particle states with  $k > 1$ , and neither from single particle nor number state populations. Consequently, none of the estimates (6,7,9) provides a tight approximation of the states' actual trace distance  $D(\rho_S, \sigma_S)$ , which exhibits a weak revival at  $t \approx 74000 \mathcal{L}^2$  due to the partially overlapping return of particles into the system's ground and first excited state [see also Fig. 2(a)]. Finally, the results in Fig. 3(b,c) emphasize that  $P_{\text{est}}^u$  – by construction – only guarantees a tight upper bound for  $D(\rho_S, \sigma_S)$  if either  $\rho_S$  or  $\sigma_S$  is sufficiently close to the many-particle vacuum state.

Many-body quantum non-Markovianity as quantified by the backflow of information is thus indeed physically anchored to the particle flow. Yet, not always can distinctive information be simply detected by single particle

population probabilities or other single particle observables, nor by number state populations, since these do not fully discriminate the intricate information content of general many-particle states.

The authors thank Heinz-Peter Breuer and Moritz Richter for fruitful discussions. J. B. thanks the Studienstiftung des deutschen Volkes for support. C. D. acknowledges the Georg H. Endress foundation for financial support.

---

[1] H.-P. Breuer, E.-M. Laine, J. Piilo, and B. Vacchini, Colloquium: Non-Markovian dynamics in open quantum systems, *Rev. Mod. Phys.* **88**, 021002 (2016).

[2] C. Cohen-Tannoudji, J. Dupont-Roc, and G. Grynberg, *Atom-Photon Interactions – Basic Processes and Applications* (Wiley-VCH Verlag, 2004).

[3] A. R. Kolovsky, Number of degrees of freedom for a thermostat, *Phys. Rev. E* **50**, 3569 (1994).

[4] A. Buchleitner and A. R. Kolovsky, Interaction-induced decoherence of atomic Bloch oscillations, *Phys. Rev. Lett.* **91**, 253002 (2003).

[5] P. Rebentrost, R. Chakraborty, and A. Aspuru-Guzik, Non-Markovian quantum jumps in excitonic energy transfer, *J. Chem. Phys.* **131**, 184102 (2009).

[6] M. Walschaers, J. Fernandez-de Cossio Diaz, R. Mulet, and A. Buchleitner, Optimally designed quantum transport across disordered networks, *Phys. Rev. Lett.* **111**, 180601 (2013).

[7] H.-B. Chen, N. Lambert, Y.-C. Cheng, Y.-N. Chen, and F. Nori, Using non-Markovian measures to evaluate quantum master equations for photosynthesis, *Sci. Rep.* **5**, 12753 (2015).

[8] F. Levi, S. Mostarda, F. Rao, and F. Mintert, Quantum mechanics of excitation transport in photosynthetic complexes: a key issues review, *Rep. Prog. Phys.* **78**, 082001 (2015).

[9] J. J. Roden, D. I. G. Bennett, and K. B. Whaley, Long-range energy transport in photosystem ii, *J. Chem. Phys.* **144**, 245101 (2016).

[10] C. A. Rozzi, S. M. Falke, N. Spallanzani, A. Rubio, E. Molinari, D. Frida, M. Maiuri, G. Cerullo, H. Schramm, J. Christoffers, and C. Lienau, Quantum coherence controls the charge separation in a prototypical artificial light-harvesting system, *Nat. Commun.* **4**, 1602 (2013).

[11] F. Meinert, M. J. Mark, E. Kirilov, K. Lauber, P. Weinmann, M. Gröbner, and H.-C. Nägerl, Interaction-induced quantum phase revivals and evidence for the transition to quantum chaotic regime in 1d atomic Bloch oscillations, *Phys. Rev. Lett.* **112**, 193003 (2014).

[12] P. Malý, J. M. Gruber, R. J. Cogdell, T. Mancal, and R. van Grondelle, Ultrafast energy relaxation in single light-harvesting complexes, *Proc. Nat. Ac. Sci. U.S.A.* **113**, 2934 (2016).

[13] M. Wittemer, G. Clos, H.-P. Breuer, U. Warring, and T. Schaetz, Measurements of quantum memory effects and its fundamental limitations, *Phys. Rev. A* **97**, 020102(R) (2018).

[14] L. Bruder, U. Bangert, M. Binz, D. Uhl, and F. Stienke-

meier, Coherent multidimensional spectroscopy in the gas phase, *J. Phys. B* **52**, 183501 (2019).

[15] B. Wittmann, F. A. Wenzel, S. Wiesneth, A. T. Handler, M. Drechsler, K. Kreger, J. Köhler, E. W. Meijer, H.-W. Schmidt, and R. Hildner, Enhancing long-range energy transport in supramolecular architectures by tailoring coherence properties, *J. Am. Chem. Soc.* **142**, 8323 (2020).

[16] M. M. Wolf, J. Eisert, T. S. Cubitt, and J. I. Cirac, Assessing non-Markovian quantum dynamics, *Phys. Rev. Lett.* **101**, 150402 (2008).

[17] H.-P. Breuer, E.-M. Laine, and J. Piilo, Measure for the degree of non-Markovian behavior of quantum processes in open systems, *Phys. Rev. Lett.* **103**, 210401 (2009).

[18] A. Rivas, S. F. Huelga, and M. B. Plenio, Entanglement and non-Markovianity of quantum evolutions, *Phys. Rev. Lett.* **105**, 050403 (2010).

[19] B. Vacchini, A. Smirne, L. E.-M., J. Piilo, and H.-P. Breuer, Markovianity and non-Markovianity in quantum and classical systems, *New J. Phys.* **13**, 093004 (2011).

[20] A. Rivas, S. F. Huelga, and M. B. Plenio, Quantum non-Markovianity: characterization, quantification and detection, *Rep. Prog. Phys.* **77**, 094001 (2014).

[21] D. Chruscinski and S. Maniscalco, Degree of non-Markovianity in quantum evolution, *Phys. Rev. Lett.* **112**, 120404 (2014).

[22] I. de Vega and D. Alonso, Dynamics of non-Markovian open quantum systems, *Rev. Mod. Phys.* **89**, 015001 (2017).

[23] H. Häffner, W. Hänsel, C. F. Roos, J. Benhelm, D. Chekalakar, M. Chwall, T. Köder, U. D. Rappel, M. Riebe, P. O. Schmidt, C. Becher, O. Gühne, W. Dür, and R. Blatt, Scalable multi particle entanglement of trapped ions, *Nat.* **438**, 643 (2005).

[24] P. M. Preiss, J. H. Becher, R. Klemt, V. Klinkhamer, A. Bergschneider, N. Define, and S. Jochim, High-contrast interference of ultra cold fermions, *Phys. Rev. Lett.* **122**, 143602 (2019).

[25] V. A. Benderskii and E. I. Kats, Coherent oscillations and incoherent tunneling in a one-dimensional asymmetric double-well potential, *Phys. Rev. E* **65**, 036217 (2002).

[26] S. Hunn, K. Zimmermann, M. Hiller, and A. Buchleitner, Tunneling decay of two interacting bosons in an asymmetric double-well potential: A spectral approach, *Phys. Rev. A* **87**, 043626 (2013).

[27] S. Hunn, *Microscopic theory of decaying many-particle systems* (Dissertation, Albert-Ludwigs-Universität Freiburg, 2013).

[28] J. Brugger, C. Dittel, and A. Buchleitner, in preparation.

[29] S. Bartels, *Numerical Approximation of Partial Differential Equations* (Springer, 2016).

[30] J. Sun and A. Zhou, *Finite Element Methods for Eigenvalue Problems* (CRC Press, 2017).

[31] P. Bocchieri and A. Loinger, Quantum recurrence theorem, *Phys. Rev.* **107**, 2 (1957).

[32] J. A. Yeazell and C. R. Stroud Jr., Observation of fractional revivals in the evolution of a Rydberg atomic wave packet, *Phys. Rev. A* **43**, 5153 (1991).

[33] F. Schwabl, *Advanced Quantum Mechanics* (Springer-Verlag, 2008).

[34] M. Walschaers, Signatures of many-particle interference, *J. Phys. B: At. Mol. Opt. Phys.* **53**, 043001 (2020).

[35] M. Walschaers, *Efficient Quantum Transport* (Dissertation, Albert-Ludwigs-Universität Freiburg, 2016).

- [36] A. J. Leggett, Bose-Einstein condensation in the alkali gases: some fundamental concepts, *Rev. Mod. Phys.* **73**, 307 (2001).
- [37] K. Sakmann, K. I. Streltsov, O. E. Alon, and L. S. Cederbaum, Reduced density matrices and coherence of trapped interacting bosons, *Phys. Rev. A* **78**, 023615 (2008).
- [38] M. A. Ruskai, Beyond strong subadditivity? Improved bounds on the contraction of generalized relative entropy, *Rev. Math. Phys.* **6**, 1147 (1994).
- [39] A. Nielsen and B. Chuang, *Quantum Computation and Quantum Information* (Cambridge University Press, 2000).
- [40] The experimentally feasible bounds (5-9) are designed to witness non-Markovian behavior: any two points in time  $t_0 < t_1$  for which either  $P_{\text{est}}^u(t_0) < P_{\text{est}}^{\ell}(t_1)$  or  $P_{\text{est}}^u(t_0) < D[\rho_S(t_1), \sigma_S(t_1)]$  imply a temporally increasing trace distance  $D(\rho_S, \sigma_S)$ , and therefore – by definition – non-Markovian behavior.
- [41] Note that, in contrast to all previous examples, these two states are not entirely orthogonal, with an initial trace distance of  $D[\rho_S(0), \sigma_S(0)] = 0.95 < 1$ .